Gene Duplication, Horizontal Gene Transfer, and Trait Trade-offs Drive Evolution of Post-Fire Resource Acquisition in Pyrophilous Fungi

Ehsan Sari[1], Dylan J. Enright[1], Maria Ordonez[1], Steven D. Allison[3], Peter M. Homyak[2], Michael J. Wilkins[4], Sydney I. Glassman[1*]

[1]Department of Microbiology and Plant Pathology, University of California, Riverside, CA, U.S.A.

[2]Department of Environmental Sciences, University of California, Riverside, CA, U.S.A.

[3]School of Biological Sciences, University of California, Irvine, CA, U.S.A.

[4]Department of Soil and Crop Sciences, Colorado State University, Fort Colins, CO, U.S.A

*Corresponding authors: sydneyg@ucr.edu and ehsansari@gmail.com

Author Contributions: S.I.G. designed the research, S.I.G, S.D.A., M.J.W. and P.M.H. acquired funding, E.S., D.J.E., and M.O. performed the culturing, molecular, and biophysical assays work. E.S. assembled and annotated fungal genomes, analyzed the data, and made figures. E.S. wrote the first draft of the paper with edits and contributions from all co-authors.

Competing Interest Statement: The authors declare no conflict of interest.

Classification: Major: Biological Sciences, **Minor:** Ecology

Keywords: Pyrophilous fungi, Comparative genomics, Aromatic carbon degradation, Nitrogen acquisition, Trait-trade-off

This PDF file includes:

Main Text

Figures 1 to 4

Abstract

Wildfires significantly alter soil carbon (C) and nitrogen (N), reducing microbial richness and biomass, while selecting for "fire-loving" pyrophilous microbes that drive post-fire nutrient cycling. However, the genomic strategies and functional trade-offs (balancing gains in one trait with costs in another) underlying the traits that enable pyrophilous microbes to survive and thrive post-fire are virtually unknown. We hypothesized that pyrophilous fungi employ specialized genomic adaptations for C and N cycling, with evolutionary trade-offs between traits governing aromatic C degradation, N acquisition pathways, and rapid growth. To test these hypotheses, we performed complementary comparative genomics, transcriptomics after pyrogenic organic matter amendment, and growth rate bioassays for 18 pyrophilous fungi from five Ascomycota (Eurotiales, Pleosporales, Sordariales, Coniochaetales, and Pezizales) and three Basidiomycota (Agaricales, Holtermaniales, and Geminibasidiales) orders isolated from burned soils. We found a dramatic trait trade-off between fast growth and number of genes responsible for aromatic C degradation, implying burned environments select for metabolically costly genes despite their evolutionary cost. We used the comparative genomics framework to evaluate genomic signatures of evolution and found that either gene duplication and somatic mutation, or recombination via sexual reproduction, were the primary drivers of fungal genomic variation in aromatic C degradation and N acquisition genes. Finally, we identified cross-kingdom bacterial to fungal horizontal gene transfer as a secondary strategy producing novel aromatic C degradation genes. Overall, we found that trait trade-offs and genome evolutionary strategies are key drivers that may predict the persistence and contribution of pyrophilous fungi to global C and N cycling.

Significance statement

Wildfires affect large tracts of the terrestrial biosphere, and while much is understood about plant adaptations to fire, here we uncovered for the first time genomic adaptations in fungi that can be modeled to predict impacts on global C and N cycling. We tested theorized trait trade-offs, and showed with genomics and bioassays how evolutionary trade-offs, like prioritizing aromatic C degradation at the expense of rapid growth, enable pyrophilous fungi to thrive post-fire. Further, we advance fungal genomics, and reveal the importance of mechanisms like gene duplication, sexual reproduction, and cross-kingdom horizontal gene transfer for enabling adaptation and evolutionary diversification in fungi. Finally, we identify fungi that may be useful inoculants to enhance recovery of polluted or burned soils.

Introduction

Wildfires are increasing in severity and intensity (1), consuming nearly 4% of Earth's land surface (~464 M ha) every year (2), and altering the processes that govern the cycling and availability of carbon (C) and nitrogen (N) (3, 4). Wildfires also affect soil microbes (5, 6), altering their composition, function, and abundance. Fires reduce microbial richness and biomass, but they also promote specific taxa of pyrophilous "fire-loving" fungi (7), with uncertain effects on soil C and N cycling (4, 8). In particular, fires increase soil N availability (9) and generate complex charcoal-derived pyrogenic organic matter (PyOM) (10), which pyrophilous fungi can degrade. Despite these important biogeochemical roles, the genomic strategies and evolutionary trade-offs that enable pyrophilous fungi to survive and thrive post-fire are largely unknown.

Due to energetic costs and evolutionary constraints, trait trade-offs may limit fungal adaptation to post-fire biogeochemistry. Investment in certain traits, such as rapid growth or thermotolerance, could limit

resource allocation to others like nutrient acquisition (11–13). Drawing from plant ecological theory and Grime's C-S-R (Competitor-Stress tolerator-Ruderal) model (14), we previously proposed that pyrophilous microbes either excel at acquisition of post-fire resources such as high N or aromatic C in PyOM (competitors), thermotolerance (stress tolerators), or rapid growth in absence of competitors (ruderals) (12, 15). Investigating trait trade-offs provides insight into how fungi balance metabolic costs with ecological demands, which can result in a valuable framework for understanding and predicting microbial diversity and functions (11). Yet, empirical tests of these hypotheses remain scarce in microbial ecology. Trade-offs between stress tolerance, fast-growth, and C acquisition traits have been demonstrated in wood decaying fungi (16, 17), but not in other groups. Tests on cultures are a key step to determine whether these hypothesized trade-offs exist in pyrophilous fungi, with important implications for predicting global C and N cycling as fires continue to influence large tracts of the terrestrial biosphere.

Comparative genomics is an ideal approach to assess the genomic evolution and adaptations of pyrophilous fungi. Fungal genomes evolve through several mechanisms, including gene duplication, polyploidy, sexual reproduction, horizontal gene transfer (HGT), and transposable elements (TEs), all of which contribute to fungal functional and ecological diversity (18). Further, the unique prominent dikaryotic phase in Basidiomycota can lead to genomic novelty (19). Previous comparative analyses on several mushroom-forming taxa from Pezizales and Agaricales have revealed unique genomic signatures in pyrophilous fungi, notably, expansions in gene families related to stress response, carbohydrate metabolism, and secondary metabolite biosynthesis (20, 21). Yet, further research is needed to address potential trade-offs between these and other ecological or physiological traits.

We hypothesize that four key mechanisms–trait trade-offs, gene duplication, HGT, and sexual recombination–have driven the development of fire-associated traits in pyrophilous fungi. Trait trade-offs may have shaped fungal specialization, balancing investments in rapid growth, thermotolerance, and resource acquisition to maximize fitness in fire-disturbed ecosystems. Gene duplication combined with mutations, which is a major source of adaptation in fungi (22), likely plays a central role by expanding enzymatic gene families involved in PyOM degradation and N acquisition, enhancing metabolic versatility in post-fire environments. HGT, which can expand capacity and adaptation (23), may contribute to the acquisition of novel aromatic C degradation and N acquisition genes, enabling more efficient resource utilization and providing a competitive advantage in nutrient-limited post-fire soils. Finally, recombination during sexual reproduction could further increase genetic diversity by creating new combinations of alleles that optimize fungal responses to nutrient pulses and environmental stressors.

Here, we leveraged a large and diverse culture collection of pyrophilous fungi isolated primarily from post-fire mushrooms and soils across California (24) to identify genomic traits and trade-offs driving rapid post-fire colonization and persistence. We combined an *in-situ* growth assay with comparative genomics based on high quality, contiguous genomes of 18 pyrophilous fungi from orders of five Ascomycota and three Basidiomycota and found a dramatic trade-off between fast growth and genes encoding aromatic C degradation. Complementary transcriptomics analysis of four pyrophilous fungal isolates from four orders to PyOM amendment across time further suggested that energetic costs of transcriptional regulation contribute to observed trait trade-offs. Overall, we propose two major genome evolution strategies that underlie the pyrophilous fungal adaptation to post-wildfire environments: one relying on gene duplication and somatic mutation (e.g., in Eurotiales) and the other on sexual recombination (e.g., in Pezizales and Agaricales). Excitingly, we identified putative cross-kingdom

horizontal gene transfer from bacteria to fungi as a rare third strategy (e.g., in Coniochaetales and Eurotiales) to enhance genetic diversity beyond the constraints of the gene pool. By generating new high-quality reference genomes for seven pyrophilous fungi, we advance understanding of fungal genome evolution, in general, as well as expand existing genomic research on pyrophilous fungi from two (20, 21) to eight fungal orders. Our findings support the hypothesis that trait trade-offs shape ecological function, with implications for global C and N cycling, and for creating microbial inoculants capable of breaking down polycyclic aromatic hydrocarbons that pollute many environments including burned soils.

Results

Genome assembly and gene annotation statistics: We generated 18 high-quality, contiguous fungal genomes from five Ascomycota orders (Coniochaetales, Eurotiales, Pezizales, Pleosporales, Sordariales) and three Basidiomycota orders (Agaricales, Geminibasidiales, Holtermanniales), which are all abundant in post-fire environments across a variety of fire-prone ecosystems (12, 15, 25), primarily from cultures isolated from burned soils and mushrooms following California wildfires (Table S1). We obtained 6.5-213 Gb of PacBio HiFi sequencing per genome with read N50 ranging from 5,429-10,028 bp providing 21-521X genome coverage (Table S2). Genome sizes ranged from 16.6 to 61.6 Mb, from 7 to 49 contigs, and contig N50 of 1.1 to 9.2 Mb (Table S3). Scaffolding with Masurca improved the contiguity of *Morchella eximia* (reduced number of contigs from 58 to 42), *Tricharina praecox* (from 52-41), and *Pholiota brunnescens* (from 53 to 49) assemblies. It also significantly improved contiguity of *N. discrete* E-DF3 (reduced number of contigs from 25 to 7) and *N. sp.* E-DF1 (from 41-23) genomes, where we used the chromosome-level assembly *of N. discrete* FGSC8579 as a reference.

We found that 16/18 of our genomes were monokaryotic, with 14 being Ascomycota, and the 2 Basidiomycota yeasts, *Basidioascus undulatus* and *Holtermanniella festucosa,* being functionally monokaryotic due to the low number of heterozygous SNPs (Table S4). However, the filamentous Basidiomycota, *Lyophyllum atratum* and *Pholiota brunnescens*, had a large number of heterozygous SNPs, suggesting that they are dikaryotic and must be treated as phased genomes (Supplementary Result 1 and Table S4). We also observed internuclear genome re-arrangement after the alignments of two haplotypes of *P. brunnescens* (Fig S1A) and *L. atratum* genomes (Fig S1B).

We also assembled 21 to 267 Kb-sized mitochondrial genomes with most isolates in a single contig (Table S5). Gene annotation guided by 2-15 million RNA-Seq paired-end reads per isolate enabled the identification 7,097-16,135 protein-coding genes per genome (Table S6). We sequenced the first genomes for 11 of our fungal isolates, with 6 providing completely novel reference genomes (Table S3, Figs. S2, S3), and provide more contiguous assemblies for 7 of them (20, 21, 26).

Trade-off between aromatic C degradation gene composition and fast growth: We paired genomes with biophysical assays to test if enrichment of aromatic C degradation and N acquisition genes trade off with growth on Malt Yeast Extract Agar (MYA) and PyOM media made from wildfire charcoal. We observed large variations in the enrichment of aromatic C degradation and N acquisition genes among pyrophilous fungal orders where Eurotiales had the most genes, followed by Pleosporales, then Coniochaetales and the lowest in Sordariales, Pezizales and Agaricales (Results S2; Fig. S4). We found that in general the Sordariales and Pezizales had the fastest growth whereas Eurotiales had the slowest growth (Fig. 1A), with a significant positive correlation between hyphal extension on MYA and PyOM media ($r=0.82$, $P=0.0001$; Fig. 1B). There was a dramatic trade-off between fast growth and enrichment

158 of post-fire resource acquisition genes as indicated by strong, significant negative correlations (r=0.53-
159 0.78, *P*=0.0001-0.05) between MYA or PyOM HE rates and the number orthologues of most aromatic C
160 degradation genes (Fig. 1B). The microbial pathways involved in the decomposition of aromatic C in
161 PyOM primarily include naphthalene degradation, catechol meta- and ortho-cleavage, and
162 protocatechuate meta- and ortho-cleavage (26–28). Fungi transform aromatic C into intermediates such
163 as catechol, protocatechuate, and benzoyl-CoA, followed by conversion to secondary intermediates such
164 as acetyl-CoA, succinyl-CoA, and pyruvate through the bKA pathway (29). Interestingly, the number of
165 *pcaF* orthologues from the bKA pathway, *mhpD* from the catechol metacleavage pathway, and *catB* from
166 the catechol orthocleavage pathway were negatively correlated solely with HE on PyOM media. Contrary
167 to our hypothesis, the correlation between N acquisition orthologue number and HE on both media
168 types was insignificant (Fig. 1B).

169 **Role of gene duplication in aromatic C degradation and N acquisition orthologues enrichment:** We
170 performed comparative genomic analysis using Orthofinder by adding 38 genomes of sister species with
171 publicly available genomes to 16 pyrophilous isolates from our study within six fungal orders (Table S8).
172 We excluded Geminibasidiales (*B. undulatus*) and Holtermanniales (*H. festucosa*) since they are the only
173 genomes sequenced from those orders. We tested the contribution of gene duplication to gene
174 enrichment by mining the Orthofinder output of the 54 genomes for the composition of 18 aromatic C
175 degradation and 4 N acquisition orthologues (Table S9). We found significant ($P < 0.05$) phylogenetic
176 signals for the enrichment of all aromatic C and N acquisition genes after normalization of gene count to
177 the total proteome size of each genome (Table S7). Orthofinder partitioned duplication events to the
178 current species (pyrophilous and their sister species) and their common ancestors (named arbitrarily by
179 Orthofinder as N0-N51) in the species tree, providing insights into the duplication event history during
180 evolution.

181 We inferred two distinct groups at the N2 common ancestor. The first group, containing the Eurotiales,
182 Pleosporales, Sordariales, and Coniochaetales, had more aromatic C degradation orthologues, while the
183 second group with Pezizales and Agaricales had fewer orthologues (Fig. 2). To test if more than one
184 major duplication event led to the enrichment seen in the first group, we compared the common
185 ancestors descended from N2. We found that the duplication rate at N6–the ancestor of Eurotiales,
186 Pleosporales, Sordariales, and Coniochaetales–was 4X higher than at the concurrent node N5, which also
187 descends from N2 and gave rise to the Pezizales and Agaricales. Meanwhile, N11 containing Sordariales
188 and Coniochaetales, experienced a decline in duplication events, while N10 containing the Eurotiales and
189 Pleosporales, and N18, the common ancestor of all contemporary Eurotiales maintained large
190 duplication events. Within Eurotiales, the common ancestor of *Penicillium* at N36 had 10X higher
191 duplication than the common ancestor of *Aspergillus* at N37. We found 36 genes-species combinations
192 with significantly ($P < 0.05$) higher gene enrichment in pyrophilous than non-pyrophilous sister species
193 (marked with blue rectangles in Fig. 2).

194 For the two dikaryotic genomes, we found that 84% of aromatic C and N acquisition genes in *P.*
195 *brunnescens* and 54% in *L. atratum* had copies in both haplotypes (Supplementary File 1), suggesting the
196 contribution of both nuclei to the genomic enrichment. *L. atratum* had duplication in one of the
197 haplotypes for 19% of aromatic C and N acquisition genes contributing further to the overall gene
198 enrichment; however, no haplotypic duplication was observed for *P. brunnescens*. Internuclear gene
199 presence/absence variation was 9% for *P. brunnescens* and 6% for *L. atratum*.

Horizontal gene transfer involved in the higher enrichment of *catA*: Considering the phylogenomic relatedness of orders and reduced duplications events at N11 (Fig. 2), we expected both Coniochaetales and Sordariales to convergently evolve to lower number of aromatic C degradation and N acquisition orthologues than Eurotiales and Pleosporales. However, Coniochaetales species had notably more orthologues like catechol-1,2-dioxygenase (*catA*) from the bKA pathway than Sordariales, suggesting that gene duplication is not the only cause of aromatic C degradation and N acquisition orthologue enrichment.

We used six methods to test for HGT. First, we examined the gene trees of *catA* orthologues and identified OG0001245, an orthogroup carrying 63 *catA* orthologues. This lent support for HGT in the pyrophilous species *Coniochaeta hoffmannii*, *Penicillium atrosanguineum*, and *Rasamsonia columbiensis* (Fig. 3A), since each had two paralogues of *catA*, one of which clustered distantly from the orthologues of their sister taxa. Gene CH_06113.t1 from *C. hoffmannii* was clustered distantly from its paralogue CH_10993.t1, and close to an orthologue from *P. atrosanguineum* (PR_10622.t1). Gene PR_10622.t1 from *P. atrosanguineum* was clustered distantly from all the other Eurotiales orthologues including its paralogue PR_04517.t1. Gene RC_00189.t1 formed a distinct cluster with an orthologue from *R. emersonii* (XP_013325789.1) close to the Pezizales orthologues, while its paralogue RC_0097.t1 was clustered with the other Eurotiales orthologues. Due to the lack of identity by descent, we propose that CH_06113.t1, PR_10622.t1, and RC_00189.t1 were introduced through HGT.

Second, we used multiple sequence alignment to align the protein sequences of the three HGT candidates and their native paralogues, and the resulting phylogenetic tree supported the distinction between the HGT candidates and their native paralogues (Fig. S5). We found a large deletion in CH_06113.t1, making it distinct from all the other five proteins (i.e., its native paralogue CH_10933.t1). Third, since previous research indicated that HGT introduced genes had lower transcription than their native counterparts (30), we examined their transcription levels and found that all three candidate HGT genes had lower transcripts per million (TPM) values than their native counterparts (Fig. 3B). Fourth, we noted that previous research found that HGT genes accumulate higher nucleotide polymorphisms than their native paralogues (31). We then use variation in sister taxa orthologues as a baseline for comparison, and we found higher numbers of nucleotide polymorphisms between orthologues of sister taxa and HGT candidates than their native paralogues (Fig. 3C). The difference was often larger for non-synonymous nucleotide polymorphisms (polymorphisms leading to protein amino acid changes).

We then search for the co-localization of Transposable Elements (TE) with HGT candidates and found a Ty3-line (Gypsy) Long Terminal Repeat (LTR) retrotransposon of ~18 kb spanning CH_06113.t1 and the two neighboring genes (Fig. S6). Finally, for our sixth method, we used a complementary analysis of pyrophilous bacterial genomes to examine the possibility of cross-kingdom HGT from bacteria to fungi. The BLAST search against the Swiss-Prot database described CH_06113.t1 as “similar to hqdA Intradiol ring-cleavage dioxygenase hqdA (*Aspergillus niger*)”, and one of the neighboring genes as “similar to tftE Maleylacetate reductase (*Burkholderia cepacia*)”. When the protein sequence of CH_06113.t1 was used as an inquiry for NCBI BLASTP search against prokaryotes gene bank, we found several orthologues. We retrieved the protein sequences of the top 20 blast hits based on the percentages of sequence identity and query coverage and combined with the protein sequences of 20 fungal orthologues, and an orthologue we found on a conjugative plasmid of *Noviherbaspirillum soli,* a pyrophilous bacterial species we isolated from the same location as *C. hoffmannii*, for phylogenetic analysis. We found that the bacterial orthologues formed a distinct cluster from those of fungi in the phylogenetic tree, except for

243 the *N. soli* plasmid orthologue that clustered with CH_06113.t1, suggesting a candidate HGT from *N. soli*
244 to *C. hoffmannii* (Fig. S7). Despite closest phylogenetic relatedness, we still found phylogenetic distances
245 between the plasmid and the candidate HGT genes (Fig S7), which could suggest an ancient transfer and
246 an independent accumulation of mutations in fungi and bacteria over the course of evolution.

247 **Role of sexual reproduction in high variation in aromatic C and N acquisition genes:** We tested if sexual
248 recombination contributed to the genetic variation in aromatic C and N acquisition genes in pyrophilous
249 fungi. To achieve that we measured nucleotide substitution rates across taxa, under the expectation that
250 lineages with regular sexual reproduction should exhibit higher substitution rates than predominantly
251 asexual species. We examined synonymous (S) and nonsynonymous (NS) nucleotide substitution rates
252 separately to distinguish neutral mutation rates from adaptive selection pressures to determine whether
253 variation in the nutrient acquisition pathways arose from selection for metabolic specialization (e.g., in
254 aromatic C degradation) or neutral diversification processes. To facilitate the visualization of results, we
255 selected one orthogroup from each of the examined pathways (Table S9).

256 We found significant ($P < 0.05$) phylogenetic signal for the number of nucleotide substitutions
257 normalized to the total proteome size of all the examined orthogroups (Table S10). Eurotiales had
258 consistently high numbers of S and NS substitutions across all pathways (Fig. 4); however, Eurotiales had
259 the lowest overall difference between pyrophilous and non-pyrophilous sister species, in line with strong
260 phylogenetic signal. Pezizales species exhibited comparable and sometimes higher S and NS
261 substitutions than Eurotiales, despite having remarkably lower gene duplication events (Figs. 2; S4). Two
262 Pezizales isolates, *Peziza echinospora* and *Geopyxis carbonaria*, ranked highest in the substitution
263 number of the catechol metacleavage and naphthalene degradation orthogroups (Fig. 4).

264 To distinguish pyrophilous adaptations from phylogenetic relatedness, we compared pyrophilous fungi
265 and their non-pyrophilous sister taxa and found that some pyrophilous fungi exhibited significantly ($P <$
266 0.05) higher nucleotide substitutions in aromatic C degradation genes than their sister taxa. We found
267 that across 38 orthogroups-species combinations (shown with asterisk in Fig. 4) where nucleotide
268 polymorphism differed between pyrophilous and non-pyrophilous species, with 29 showing higher
269 nucleotide variation in pyrophilous species. *Aspergillus cf. felis* had significantly higher S and NS
270 substitutions in the catechol orthocleavage, catechol metacleavage, and naphthalene degradation
271 orthogroups than all the other sister *Aspergillus* species, and *Alternaria* sp. had higher substitutions in
272 the catechol orthocleavage, bkA pathway, and naphthalene degradation orthogroup than all the other
273 *Alternaria* species (Fig. 4). *Coniochaeta hoffmannii* had the highest NS substitutions in the bKA pathway
274 orthogroups within the Coniochaetales and also ranked highest among all 53 taxa.

275 **Dikaryotic internuclear variation contributes to nitrate-reductase (narG-narZ) variation:** The dominant
276 dikaryotic phase common in Basidiomycota where two genomes exist in two separate nuclei in each cell
277 allows them to take advantage of diploid genomes (e.g., increased genetic diversity and protection
278 against deleterious mutations) while reducing the tension between unrelated haploid genomes (32). We
279 leveraged our high-quality assemblies to establish phased genomes for the dikaryon *L. atratum* to test
280 the contribution of internuclear variation to higher nucleotide substitution observed in nitrate-reductase
281 (*narG-narZ*) genes (Fig. 4). We found a high number of substitutions in the Agaricales OG0000632
282 orthogroup described as *narG-narZ*. We selected an OG0000632 orthologue of *Lyophyllum atratum*
283 (LA_01440.t1) and aligned two haplotypes representing the sequences of two nuclei and found 16
284 nucleotide polymorphism sites in the exonic regions (Fig. S8). We then aligned RNA-seq reads to one

285 haplotype as a reference and observed reads derived from both haplotypes at a nearly 1:1 ratio at all 16
286 polymorphism sites, indicating that the two haplotypes were transcribed in equilibrium. This suggests
287 that internuclear variation drove the higher number of substitutions in *narG-narZ* in *L. atratum*.

288 **Transcriptome response of selected pyrophilous fungi to PyOM treatment:** We performed
289 transcriptomics at 0, 2, 4, 24 and 48 hours after PyOM amendment to assess how PyOM affected gene
290 transcription across time for 4 isolates. We selected *Coniochaeta hoffmannii*, *Penicillium*
291 *atrosanguineum*, *Morchella eximia,* and and *Pholiota brunnescens* representing four orders with distinct
292 levels of aromatic C degradation and N acquisition gene enrichment. We found that orthologues of 14
293 genes in *C. hoffmannii* (Fig. S9), 21 in *P. atrosanguineum* (Fig. S10), 17 in *M. eximia* (Fig. S11), and 15 in *P.*
294 *brunnescens* (Fig. S12) were differentially transcribed in response to PyOM treatment. There was a
295 common set of aromatic C degrading genes showing differential transcription in all fungi, for example
296 the catA orthologues. In contrast, transcription of certain gene orthologues like *nahB_doxE* only
297 positively responded to PyOM only in *P. atrosanguineum* (Fig. S10) and *M. eximia* (Fig. S11), despite
298 being present in all four species (Fig. 2). In terms of N acquisition, *narG-narZ* was induced in all four
299 species and *nirK* was induced in all but *C. hoffmannii*.

300 **Discussion**

301 We provided an experimental test of ecological theory to reveal a fundamental trait trade-off between
302 ability to grow fast and acquire post-fire resources in pyrophilous fungi. This genomic balancing act
303 underpins the selective advantage of carrying larger suites of aromatic C degradation genes in wildfire-
304 impacted environments. Our findings suggest that gene duplication and mutations represent one route
305 for generating variation within aromatic C degradation and N acquisition genes in pyrophilous fungi (e.g.,
306 in Eurotiales), while recombination via sexual reproduction and internuclear variation offer an
307 alternative mechanism (e.g., in Pezizales and Agaricales). We also show evidence that ancient bacterial
308 to fungal cross-kingdom HGT contributes to genetic novelty in PyOM degradation in pyrophilous fungi
309 (e.g., in Coniochaetales and Eurotiales). Finally, we found stringent transcriptional regulation of aromatic
310 C and N acquisition genes in four distantly related pyrophilous fungi, showing low baseline transcription
311 in regular media but strong induction following PyOM treatment. This finding suggests that the energetic
312 costs of transcription contribute to observed trait trade-offs and that transcriptional responses to PyOM
313 are shaped less by phylogeny and more by shared ecological adaptation to post-fire environments. We
314 integrate comparative genomics, transcriptomics, and growth assays to link specific genetic changes with
315 ecological outcomes in a diverse array of understudied pyrophilous fungi that may have exceptional
316 potential as fungal inoculants for ecosystem recovery after disturbances.

317 **Microbial trait trade-offs at genomic levels:** Combining hyphal extension assays with high-quality
318 genomes of 16 filamentous pyrophilous fungal isolates, we found large, significant trade-offs between
319 fast growth and enrichment for aromatic C degradation genes. For instance, the Ascomycota order
320 Pezizales grew fast at the expense of fewer aromatic C breakdown orthologues, while Eurotiales grew
321 slowest but was enriched for aromatic C degradation. Surprisingly, we found no trade-offs between fast
322 growth and enrichment of genes for N acquisition, which may reflect that inorganic N is so prevalent
323 across post-fire ecosystems (cite) that it is not necessary to invest heavily in acquiring it, or alternatively
324 that efficient N scavenging is a widespread evolutionary pressure across most ecosystems (33). In
325 contrast, the recalcitrance of PyOM requires highly specialized enzymatic machinery (34), creating a
326 stronger metabolic cost driving the trade-off with growth. The fast-growth-aromatic C acquisition trade-

327 off observed here, along with genetic and copy number variation within the aromatic C degradation and
328 N acquisition orthologues, supports the ideas of functional diversity and specialization among
329 pyrophilous fungal lineages. The rapid growth of Pezizales species corresponds to their early successional
330 role in post-fire environments, coinciding with a surge of bioavailable nutrients from necromass (15, 35).
331 Similarly, the comparatively slower growth of Eurotiales aligns with their late successional role, where
332 enrichment of aromatic C-degrading genes likely facilitates resource acquisition from difficult to degrade
333 PyOM (36) Many Eurotiales are known for their rapid colonization of substrates (37), which made their
334 slower growth unexpected; however, it might be specific to the pyrophilous Eurotiales species we
335 examined, as evidenced by higher enrichment of aromatic C genes in pyrophilous Eurotiales and their
336 sister species than other Eurotiales. This variation in growth rates among Eurotiales highlights the
337 diverse ecological strategies within the order, ranging from fast-growing opportunists to more
338 specialized, slower-growing species adapted to specific niches like post-fire environments.

339 **New pyrophilous taxa as candidate contributors to aromatic C degradation and N acquisition:** Our
340 results suggest that three Ascomycota orders–Eurotiales, Pleosporales, and Coniochaetales–are likely
341 major players in aromatic C degradation due to gene enrichment. We know of only two prior studies
342 examining pyrophilous fungal genomes that focused on six isolates of Pezizales and three of Agaricales
343 that all formed mushrooms on burnt soil (20, 21). In contrast, Eurotiales, Pleosporales, and
344 Coniochaetales do not form macroscopic fruiting bodies but are commonly identified in microbiome
345 studies of burned soils (12, 15, 25) and we isolated them from burned soil slurries (24). The Eurotiales
346 isolates we studied included *Rasamsonia columbiensis,* which is a thermotolerant species (37) that has
347 been isolated from house dust (38), *Penicillium atrosanguineum,* which has been isolated from forest soil
348 (39), *P. antarcticum*, which was previously isolated as an endophyte from Antarctica native plants (40),
349 and *Aspergillus fellis,* also previously isolated as an endophyte (41) and from rocks (42). Endophytic fungi
350 may be potent decomposers of aromatic C due to their ability to decompose the host's dead cell wall
351 and penetrate host plant barriers while establishing endophytic relationships (43). The endophytic
352 lifestyle could be linked with post-fire survival by providing an escape mechanism, as internal
353 colonization of plant tissues, especially roots, offer insulation from extreme heat and flames, allowing
354 fungi to persist and subsequently colonize burned soil (44, 45). Pleosporales, such as *Alternaria*, are
355 adapted to a wide range of ecological niches and are ubiquitous saprobes, wide-host-range plant
356 pathogens, and plant endophytes (46). *Coniochaeta hoffmannii* is also known as a wood-decaying soil
357 fungus and a plant pathogen that was previously isolated from a car fuel reservoir and can degrade
358 polypropylene plastic (47). Eurotiales, Coniochaetales, and Pleosporales pyrophilous species,
359 characterized by enriched aromatic C degradation and N acquisition genes and extremophilic
360 adaptations to environments like Antarctic soils, fuel reservoirs, and pyrolyzed substrates, exhibit dual
361 capacities critical to post-wildfire recovery–degradation of fire-derived aromatics (e.g., polypropylene-
362 like pyrolyzed compounds), and tolerance of post-fire abiotic stressors (e.g., desiccation and UV
363 exposure). Their genomic toolkit, refined through adaptation to post-fire conditions, positions these
364 fungi as key mediators of C and N cycling in burned soils, with potential applications in restoring fire-
365 disturbed ecosystems. In contrast, the Basidiomycete pyrophilous fungi did not have as many genes for
366 aromatic C degradation, which may reflect their specialization in lignin degradation (48).

367 We assembled contiguous genomes for two basidiomycete yeasts, *Holtermanniella festucosa* from
368 Holtermanniales and *Basidioascus undulatus* from Geminibasidiales, which were both genomic orphan
369 orders. These species are novel pyrophilous fungi and have been repeatedly identified in previous

370 studies as dominant soil colonizers following wildfire (12, 15, 25, 49). However, due to the absence of
371 closely related reference genomes, we were unable to include these isolates in our comparative genomic
372 analyses.

373 **Gene duplication, an adaptation strategy to post-fire environments in pyrophilous fungi:** Our study
374 revealed that ancient gene duplication plays a crucial role in shaping the current composition of
375 aromatic C degradation and N acquisition genes in pyrophilous fungi, likely as an adaptation to frequent
376 exposures to post-fire environments. Gene duplication is a well-established mechanism for creating
377 genetic variation and functional innovation across different forms of life and especially within Kingdom
378 Fungi, where five large gene duplication bursts have been identified (50). Among our isolates, gene
379 duplications decreased throughout evolutionary history, but this decline was slower for the common
380 ancestors of the current pyrophilous species in the Eurotiales, Pleosporales, Sordariales, and
381 Coniochaetales orders. Eurotiales species showed the slowest decline, maintaining the largest repertoire
382 of aromatic C degradation genes in their contemporary forms. This slow decline leading to high load of
383 aromatic C degradation genes highlights the significant role that Eurotiales likely play in aromatic C
384 degradation, at least in fire disturbed chaparral soil, where our pyrophilous Eurotiales species were
385 isolated (24). A previous study found a correlation between gene copy numbers of ring-hydroxylating
386 dioxygenase in soil samples and degradation efficiency, highlighting the quantitative nature of microbial
387 aromatic C degradation (51). Gene duplication thus provides novel genes for higher expression and raw
388 materials for genomic novelty for functional diversification. While gene duplication affecting C and N
389 metabolism is a common evolutionary strategy in other fungi (22), our findings underscore its particular
390 importance for pyrophilous fungi supported by the significant enrichment of some genes in pyrophilous
391 vs. non-pyrophilous sister species. The higher enrichment in pyrophilous fungi despite strong
392 phylogenetic signal likely represents a specific adaptation to unique post-fire C and N resources.
393 However, we observed differing duplication frequencies between aromatic C and N acquisition genes
394 across pyrophilous fungal species supported with strong phylogenetic signal. This suggests lineage-
395 specific variations in employing gene duplication as an adaptive strategy post-fire. Previous studies also
396 suggested that pyrophilous fungi are phylogenetically conserved, with the Eurotiomycetes and
397 Pezizomycetes having more pyrophilous fungi than expected by chance (12).

398 **Enhancing genetic variation in aromatic C and N acquisition genes through ancient HGT:** Here, we
399 provide for the first time compelling evidence for an ancient HGT of a *catA* gene from bacteria to *C.* 3/18
400 pyropilous fungi, *hoffmannii, R. columbiensis* and *P. atrosanguineum.* HGT is rare in fungi, making its
401 occurrence in multiple pyrophilous species surprising and suggesting that the extreme, stress-intensive
402 post-fire environment may promote such events, analogous to how the gut environment facilitates HGT
403 (52). Our phylogenetic analyses using the *catA* orthologues in fungi, bacteria, and a plasmid gene we
404 discovered through sequencing the genome of the pyrophilous bacterium *N. soli*, suggested distinction
405 between most bacterial and fungal sequences. It is likely due to an ancient HGT event subjected to
406 distinct evolution trajectories in fungi or the conjugation of a *N. soli* plasmid gene that has a protein
407 sequence distinct from all *catA* in the bacterial kingdom. The former is supported by the presence of
408 *catA* HGT events in distantly related orders of Coniochaetales and Eurotiales, and the latter by the
409 clustering of plasmid-born *catA* with the fungal HGT candidate gene. It is possible that this gene was
410 transferred into their common ancestor and subsequently lost in some descended taxa possibly due to
411 fitness penalties. HGT from bacteria to fungi is rare but is increasingly recognized as a significant
412 mechanism for fungal genome evolution and adaptation (53). Notable examples include the transfer of

413 bacterial glycosyl hydrolases to Neocallimastigomycota rumen fungi, enhancing their ability to break
414 down plant material (54). The HGT events in aromatic C degradation genes like *catA* may have conferred
415 a novel function allowing pyrophilous fungi to outperform native soil communities in acquiring C from
416 PyOM, which might be tested with future research generating a knockout of the HGT *catA* gene in
417 pyrophilous fungi like *C. hoffmannii*. The cross-kingdom HGT of aromatic C acquisition genes is a novel
418 mechanism of adaptation in pyrophilous fungi to post-fire environments, where higher genetic variation
419 in aromatic C degrading genes is likely advantageous.

420 **Contribution of sexual recombination to pyrophilous fungal genetic variation:** Sexual recombination
421 generates novel allelic combinations and increases nucleotide diversity, whereas strictly asexual species
422 accumulate variation more slowly, potentially limiting their genetic diversity despite multiple gene
423 duplications. The number of nucleotide polymorphisms varied substantially across pyrophilous orders
424 and surprisingly did not linearly increase with the number of gene duplications. Pezizales exhibited
425 comparable, and in some cases, higher nucleotide polymorphisms than Eurotiales, despite having
426 significantly fewer gene copies. Differences in sexual reproduction frequency, which is rare among
427 Eurotiales species, with some reproducing strictly asexually (37), but common among pyrophilous
428 Pezizales species (20), may suggest two distinct mechanisms for maintaining diversity in pyrophilous
429 fungi. In fungi with limited sexual reproduction, like Eurotiales, genetic variation could be maintained
430 through gene duplication followed by somatic mutations. In contrast, genetic variation might balance
431 through sexual recombination in lineages like Pezizales with frequent sex. The high genetic variation
432 observed in aromatic C degradation and N acquisition genes could allow pyrophilous Pezizales species
433 such as *Pyronema omphalodes* to access various bioavailable C and N resources released from
434 necromass immediately post fire, explaining the rapid colonization of burned soil by *Pyronema* (15, 35).
435 The slower-growing Eurotiales pyrophilous species appear to take over later in succession (15), likely due
436 to their higher gene copies which enable them to acquire more complex aromatic C and N resources that
437 are inaccessible to pyrophilous Pezizales.

438 Despite strong phylogenetic signal, we observed significant differences between pyrophilous and non-
439 pyrophilous sister species in the number of nucleotide substitutions of some genes, particularly for
440 *Aspergillus cf. felis*, suggesting that stressful post-fire habitats can promote elevated genetic variation as
441 a strategy for adaptation (55). We identified that inter-nuclear nucleotide variation contributed to the
442 total composition of aromatic C and N acquisition genes for two dikaryotic basidiomycetes *P.*
443 *brunnescens* and *L. atratum*. We also identified internuclear variation in *L. atratum* associated with a
444 nitrate-reductase (*narG-narZ*) gene that exhibited unexpectedly high genetic variation. This finding
445 further supports the role of sexual reproduction and dikaryon formation in Basidiomycota as a
446 mechanism for enhancing genetic variation in resource acquisition genes among pyrophilous fungi.
447 Together, these results underscore multiple evolutionary strategies employed by pyrophilous fungi to
448 maintain genetic diversity and adapt to the dynamic nutrient landscapes of post-fire environments.

449 **Transcriptional changes in aromatic C and N acquisition genes in response to PyOM treatment:** In
450 addition to the RNA-sequencing for genome annotation, we performed differential gene transcription
451 across time after PyOM amendment. We selected 4 isolates, *C. hoffmannii, P. atrosanguineum*, *M.*
452 *eximia*, *P. brunnescens*, representing four different orders ranging from lower to higher gene enrichment
453 for aromatic hydrocarbons and N acquisition. We observed strong transcriptional activation of key
454 aromatic C degrading genes after PyOM treatment, indicating that expressing these pathways is
455 metabolically costly and supporting the growth trade-off demonstrated in our bioassays Our results align

with previously published results suggesting the charcoal modulating genes were differentially transcribed in two pyrophilous sister species *Pyronema omphalodes* and *P. demesticum* after PyOM treatment (20). We found aromatic C and N acquisition genes commonly transcribed in four species, suggesting partial conservation of response to PyOM in pyrophilous fungi. This pattern indicates that the transcriptional response is driven less by phylogenetic relatedness and more by shared ecological adaptation to post-fire environments. Similar patterns have been reported in soil fungi, where enzyme activity and nutrient acquisition functions remain conserved across communities despite high taxonomic variability (56).

Conclusions: Our study advances fungal genomics by expanding the genomic resources for pyrophilous fungi, including several previously uncharacterized lineages. Leveraging our large and diverse culture collection of pyrophilous fungi (cite), we use high-quality genomes and complementary transcriptomics and bioassays to conduct one of the first experimental tests of trait trade-offs in fungi. We reveal that pyrophilous fungi exhibit a striking trade-off between rapid growth and the enrichment of aromatic C degradation genes, an adaptation that likely confers a selective advantage in fire-affected soils dominated by PyOM. We also found that this trade-off did not exist for N genes, suggesting that there is less metabolic cost to invest if N acquisition machinery. Our study suggests that at least two major genome evolution strategies drive the adaptation of pyrophilous fungi to post-wildfire environments: one relying on gene duplication and somatic mutation (e.g., in Eurotiales) and the other on sexual recombination (e.g., in Pezizales and Agaricales). HGT events, as examined in *C. hoffmannii*, *R. columbiensis* and *P. atrosanguineum*, is likely a third rarer strategy enhancing genetic diversity in pyrophilous fungi beyond the gene pool barrier. Future research should investigate how these distinct evolutionary strategies influence interactions among pyrophilous fungi, prioritizing the study of newly identified species with enriched aromatic C and N acquisition genes. Collectively, our findings expand the frontier of pyrophilous fungal genomics, advance our ability to predict their roles in global C and N cycling, and identify functionally robust pyrophilous isolates that could serve as microbial inocula for post-fire soil restoration.

Materials and Methods

Fungal isolates: We leveraged our collection of pyrophilous fungi isolated primarily from post-fire mushrooms and soils across California. We included 18 pyrophilous fungal isolates from across two phyla and 8 orders (Table S1). We selected these isolates because they were abundant across a variety of fire-prone ecosystems (7, 12, 15, 25) and we expected them to exhibit a diversity of pyrophilous trait strategies (12).

High Molecular Weight (HMW) DNA Extraction and PacBio HiFi Sequencing: We extracted HMW DNA from fungal tissue with either Qiagen Genomic Tip 100/G (Qiagen, Hilden, Germany) or using a CTAB:Phenol:Chloroform method (57) if extraction with Qiagen Tips led to low DNA concentration (Table S1). See Methods S1 for fungal tissue preparation and DNA extraction details.

We then submitted DNA to the University of California Irvine Genomics Research and Technology Hub (UCI GRTH) for HiFi SMRT Bell Library Preparation and PacBio HiFi Sequencing. The sequencing library was prepared using SMRTbell template prep kit version 3.0 with the overhang barcoded adapters (PacBio, Menlo Park, USA) and sequenced on the Sequel IIe™ System (PacBio, Menlo Park, USA), except for *Neurospora sp.* E-DF1, *Neurospora discreta* E-DF3, and *Tricharina praecox*, which were sequenced

using the Revio™ system (PacBio, Menlo Park, USA). Samples were multiplexed to achieve the genome coverage ≥ 20X.

Genome Assembly Pipeline: We generated draft genome assemblies for each isolate using Hifiasm v.0.16.1-r375 (58), IPA v.1.8.0 with --no-phase command for haplotype genomes (https://github.com/PacificBiosciences/pbipa), hiCanu v.2.2 (59), Peregrine v.0.4.13 with reduction factor of 4 specified with -r 4 and window size of 64 specified with -w 64 (https://github.com/cschin/peregrine-2021?tab=readme-ov-file), and Flye v.2.9-b1774 (60). For phased assemblies of hiCanu and Hifiasm, the represented primary haplotype for haploid dikaryotic genomes were obtained using purge-dups v.1.2.6 with default parameters (https://github.com/dfguan/purge_dups). We obtained the assembly metrics using QUAST software v.5.2.0 (61), and used BUSCO software v.5.4.3 to assess assembly completeness (62). We used the most contiguous and complete assembly as a reference for scaffolding with the Masurca software v.4.1.0 SAMBA tool (63) with raw HiFi reads and then with the other inferior draft assemblies or available chromosome-level genome assemblies as inputs. We used the chromosome-level assembly of *N. discreta* FGSC8579 as reference (https://genome.jgi.doe.gov/portal/pages/projectStatus.jsf?db=Neudi1&utm_source=chatgpt.com) for scaffolding *N. discreta* E-DF3 and *N.* sp. E-DF1 genomes(63). We visualized the alignment of the HiFi reads to genome at the genomic loci where two contigs were merged through scaffolding in Integrative Genome Viewer (64). Breaks were introduced if read support was insufficient. Finally, we identified and corrected the miss-assemblies using CRAQ software v.1.0.9 (https://github.com/JiaoLaboratory/CRAQ). We found telomere repeat sequences with the FindTelomeres script (https://github.com/JanaSperschneider/FindTelomeres). We assembled the mitochondrial genome using get_organel software v.1.7.7.1 (https://github.com/Kinggerm/GetOrganelle) with the Hifiasm assembly graph as an input We identified heterozygous single nucleotide polymorphisms (SNPs) between the haplotypes of the dikaryotic genomes and phased them using HapCUT2(65). We used the number of heterozygous SNPs as a proxy for the extent of internuclear genetic variation in the basidiomycete genomes assumed to have haploid dikaryotic genomes. We also identified internuclear genomic rearrangement in haploid dikaryotic genomes by genome-wide alignment between the contigs obtained for two haplotypes using MUMmer v.4.0.1 (66).

RNA extraction and sequencing: We grew the 18 fungal isolates in three conditions: in malt yeast broth 1) at ambient temperature 2) in ambient temperature followed by a 1 hr 40 °C heat-shock, or 3) on PyOM agar plates covered with cellophane sheets at ambient temperature. In addition, we selected a subset of 4 fungal isolates (*C. hoffmannii*, *P. atrosanguineum*, *M. eximia*, and *P. brunnescens*) to test the transcriptional changes in aromatic C and N acquisition genes after PyOM amendment. The four fungal isolates were first grown in MYB medium (Methods S1) for 5 days, and the resulting biomass was harvested and exposed to PyOM liquid media (24). Samples from three biological replicates per condition were collected at 0 (before PyOM amendment), 2, 4, 24, and 48 h post PyOM treatment for RNA extraction and mRNA sequencing. Differential transcription analysis was performed using DESeq2 (67), with all time points compared against the 0 h for the calculation of fold change in transcription. Statistical significance of differential transcription was determined in DESeq2 using adjusted p-values (Benjamini–Hochberg false discovery rate < 0.05). We extracted total RNA with the E.Z.N.A.® Fungal RNA Mini Kit (Omega Bio-Tek, Norcross, U.S.A.) following manufacturer's protocol. See Methods S2 for method used for the RNA quality control. We prepared mRNA Illumina libraries using the Illumina

540 TruSeq® RNA Sample Preparation v. 2 Kit (Illumina, San Diego, USA) and sequenced on the NovaSeq 6000
541 system (Illumina, San Diego, USA) at the UCI GTRH for annotation and at the U.S. Department of Energy
542 Joint Genome Institute for the PyOM treatment experiment.

543 **Gene and TE Annotation**: We used RNA-seq data to annotate the protein-coding genes with the FunGAP
544 pipeline (68) after trimming sequencing adapters with TrimGalore v.0.6.10
545 (https://github.com/FelixKrueger/TrimGalore), and filtering to retain only reads with a Phred quality
546 score > 30 and length of ≥ 50 bp. We assigned putative sequence descriptions to protein sequences
547 predicted by FunGAP by searching with NCBI-BLASTP v.2.16.0 (https://blast.ncbi.nlm.nih.gov) against the
548 reviewed UniProtKB database (Swiss-Prot, downloaded in Aug 2023). For each protein, we extracted the
549 InterPro protein families and Gene Ontology (GO) terms (69) using InterProScan v. 5.62-94.0
550 (https://interproscan-docs.readthedocs.io/en/latest/) and the Kyoto Encyclopedia of Genes and
551 Genomes (KEGG) ontology terms using kofam_scan v.1.3.0 (https://github.com/takaram/kofam_scan).
552 We annotated the mitochondrial genes with the GeSeq online tool (https://chlorobox.mpimp-
553 golm.mpg.de/geseq.html). We annotated TEs with the Transposon Annotator "reasonaTE" tool (70) and
554 calculated the percentage of the genome annotated as TEs by dividing the number of nucleotides in the
555 annotated TE regions by the total genome length, multiplied by 100.

556 **Annotation of Aromatic C Degradation and N-acquisition Genes:** We generated Hidden Markov Model
557 (HMM) profiles for 18 aromatic C degradation and 4 N acquisition genes (Table S9) examined previously
558 (27). Aromatic C degradation genes examined belonged to meta- and ortho-cleavage for both catechol
559 and protocatechuate and naphthalene degradation pathways (26–28). According to previous studies,
560 fungi transform aromatic C into intermediates such as catechol, protocatechuate, and benzoyl-CoA,
561 followed by conversion to secondary intermediates such as acetyl-CoA, succinyl-CoA, and pyruvate
562 through the β-ketoadipate (βKA) pathway (29), so we also examined genes from the bKA pathway.

563 We also examined N acquisition genes such as nitrate and nitrite reductase whose transcription were
564 previously shown to increase after fire (71). We also included nitrous oxide reductase (*nosZ*) since high-
565 severity fires may impair the soil microbiome's capacity to convert nitrous oxide (N_2O), a potent GHG, to
566 nitrogen (N_2) gas (72), leading to elevated N_2O emission from burned soil (73). Fungi play a unique role in
567 this process. We also included *P450nor* because some fungi possess Cytochrome P450 nitric oxide
568 reductase (*P450nor*), an enzyme that catalyzes the reduction of nitric oxide (NO) to N_2O during fungal
569 denitrification (74).

570 We downloaded all protein sequences associated with each gene from NCBI, and discarded proteins
571 annotated as similar or partial in their FASTA headers. We then aligned the high-confidence protein
572 sequences of each gene using ClustalOmega v. 1.2.4 (75) with default parameters and used the
573 alignments to build HMM profiles using the hmmbuild command of HMMER v.3.4 (http://hmmer.org/).
574 We used these HMM profiles to annotate each fungal isolate's protein sequences using the hmmsearch
575 command of HMMER v.3.4, with an E-value cutoff of 1e-23. To confirm that the hmmsearch accurately
576 retrieved the orthologues of each gene, we matched the available sequence descriptions and domain
577 annotations obtained using BLAST and Interproscan with the description of proteins used as inputs for
578 building HMM profiles.

579 For basidiomycetes with dikaryotic genomes, we assessed the contribution of internuclear
580 rearrangements to the total number of aromatic C degradation and N acquisition genes by separately
581 annotating the two haplotypes of genomes assembled with HiFiasm (58) using the FunGap pipeline (68).

582 Coding sequences (CDSs) from the two haplotypes were then matched using JCVI (76). Gene
583 relationships were categorized as 1:1 (one gene in each haplotype), duplicated (more than one copy in a
584 single haplotype), or presence–absence variants (gene missing in one haplotype).

585 **Orthogroup Construction and Visualization:** We performed comparative genomic analysis of 16
586 pyrophilous fungi belonging to the 6 orders for which publicly available genomes of sister species existed
587 along with 38 sister species (Table S8) selected as described in Methods S3. We assigned genes to
588 orthogroups (clusters of orthologues across genomes) using Orthofinder v.2.5.5 (77) and used the gene
589 IDs of HMMER annotated aromatic C degradation and N acquisition genes to extract assigned
590 orthogroups from the Phylogenetic Hierarchical Orthogroups predicted for the oldest common ancestor
591 of all species (N0). We obtained the orthogroups per gene family and individual genes by creating a
592 matrix of orthologue counts per species. We visualized the sum of genes for each of naphthalene
593 degradation, catechol meta- and ortho-cleavage, protocatechuate (PCA) ortho- and meta-cleavage, and
594 N-acquisition pathways alongside the species tree generated with Orthofinder using the plotTree.barplot
595 function of Phytools (https://cran.r-project.org/web/packages/phytools/index.html) in R v.4.3.2 (78). To
596 identify gene duplication events leading to the current composition of aromatic C degradation and N
597 acquisition genes in the pyrophilous fungi, we obtained the number of gene duplication events in these
598 genes occurring at each current node (53 species) and their common ancestors from the Orthofinder
599 Gene Duplication Events reports. For dikaryotic genomes, we assessed the genome enrichment of each
600 haplotype separately (supplementary file 1) and count of gene duplication events was doubled if both
601 haplotypes carried the genes. We visualized the number of gene duplication events on the phylogenetic
602 tree alongside the orthologue counts per individual gene using iTOL software v.7 (https://itol.embl.de/).

603 We also tested the involvement of phylogenetic signals in aromatic C and N acquisition gene enrichment.
604 We normalized the gene counts by total proteome size to account for differences in genome content.
605 Using the rooted phylogenetic tree generated by Orthofinder, we quantified phylogenetic signal for each
606 gene with Pagel's λ, estimating associated likelihood-ratio test p-values using the phylosig function from
607 the R package phytools (79).

608 To test for enrichment of gene families in pyrophilous versus non-pyrophilous fungi, we implemented
609 generalized linear models (GLMs) with a Poisson distribution in R (78), using gene family counts as the
610 response variable, fungal lifestyle (pyrophilous or non-pyrophilous) as the predictor, and proteome size
611 as an offset. Significance of enrichment was assessed from the trait (pyrophilous vs. non-pyrophilous)
612 coefficient, and false discovery rate (FDR) was controlled using the Benjamini–Hochberg method.

613 **Identification of candidate HGT events:** We identified candidates for HGT events by visually inspecting
614 the putative xenologues generated by Orthofinder for outlier orthologues clustered distantly from their
615 sister species in their gene trees then validated them with the following steps. We visualized the aligned
616 protein sequences of candidate HGT genes and their corresponding native genes in the orthogroup using
617 iTOL software v.7 (https://itol.embl.de/). Next, we compared candidate HGT gene transcription levels
618 with their corresponding native genes (orthologues complying with phylogeny in the gene tree) in the
619 orthogroup. We aligned the RNA-seq reads to their corresponding fungal genome using HISAT2 v.2.2.1
620 (80). We then calculated the Transcript Per Million (TPM) values for each gene using TPMCalculator
621 v.0.0.5 (81) from the spliced alignment BAM file generated with HISAT2. Next, we calculated synonymous
622 (S) and non-synonymous (NS) nucleotide substitution rates of the HGT candidates and their
623 corresponding native genes using KaKs_Calculator v.3.0 (82). We also examined the co-localizations of

624 the loci with the candidate HGT genes and TEs by visualizing the GFF3 files containing gene and TEs
625 annotations in Integrated Genome Viewer (IGV) software v.2.15.2 (64). We also used BLASTP v.2.16.0
626 (https://blast.ncbi.nlm.nih.gov/Blast.cgi) to retrieve the protein sequences with homology to candidate
627 HGT genes within all publicly available proteins from fungi and bacteria kingdoms in NCBI gene bank for
628 phylogenetic analysis to identify potential HGT donor species. We included a *catA* gene identified on a
629 conjugative plasmid of a pyrophilous bacteria *Noviherbaspirillum soli* (from Burkhorderiales order)
630 through genome sequencing of pyrophilous bacteria (83).

631 **Measuring genetic variation among taxa in aromatic C degradation and N acquisition genes:** We
632 calculated the nucleotide substitution rate of the aromatic C degradation and N acquisition genes for the
633 53 genomes subjected to orthogroup construction with KaKs_Calculator v.3.0 (82). We visualized with a
634 heatmap generated for a single orthogroup per each of the naphthalene degradation, catechol meta and
635 ortho-cleavage, and protocatechuate meta and ortho-cleavage, and N acquisition pathways using the
636 heatmap.2 function of R v.4.3.2 (84). The presence of phylogenetic signals and the significant differences
637 between the pyrophilous and their non-pyrophilous sister species in the number of nucleotide
638 substitutions were drawn as described above for gene enrichment analysis. See Methods S4 for methods
639 examining contribution of internuclear variation in Basidiomycota to variation among aromatic C
640 degradation and N acquisition genes.

641 **Measuring trade-off between fast-growth, and aromatic C degradation and N-acquisition:** We
642 measured HE rate on MYA or PyOM media for 16 filamentous pyrophilous isolates using three biological
643 replicate plates per media type per isolate. We covered each plate with a sterile cellophane sheet (16),
644 then inoculated a 5 mm^2 radius plugs of fungal tissue into the center, then incubated at room
645 temperature with the hyphal growing edge recorded every 24 h using alternating-colored markers. After
646 3 weeks, plates were photographed, and images were imported into ImageJ v.1.54
647 (https://imagej.net/ij/) where daily extension rates were quantified in millimeters per day. We calculated
648 the pairwise Spearman's rank correlation between the HE rates on MYA and PyOM media and the
649 number of each aromatic C degradation and N acquisition orthologues of each species using the rcorr
650 function (85) and visualized using the corrplot function of R (86).

651 **Acknowledgements:** This project was funded by the Department of Energy BER Award #DE-SC0023127
652 to SIG, PMH, SDA, and MJW and United States Department of Agriculture-NIFA Award #2022-67014-
653 36675 to SIG and PMH. The RNA-seq studying transcription Post-PyOM treatment was conducted
654 through Proposal ID: 510601, DOI: 10.46936/10.25585/60012549 by the U.S. Department of Energy Joint
655 Genome Institute (https://ror.org/04xm1d337), a DOE Office of Science User Facility, supported by the
656 Office of Science of the U.S. Department of Energy operated under Contract No. DE-AC02-05CH11231.
657 We thank many individuals who contributed to the Glassman lab pyrophilous microbial culture including
658 lab managers Judy Chung and James Randolph, lab assistants Ryan Quaal and Aishwarya Veerabahu,
659 collaborators Tom Bruns and Monika Fischer, UCR PhD students Fabiola Pulido-Chavez, Arik Joukhajian,
660 Esbeiry Cordova-Ortiz, and Mark Yacoub, and UCR undergraduates Anna Nguyen, Marely Vega, Jenna
661 Maddox, Justin Diab, Wine-Jie Lipardo, Audrey Reichard, Priscilla Shultz, Jorge Ponce, and Nathan Heger.
662 We thank Jason Stajich and his lab for advice and protocols for high molecular weight DNA extraction.
663 We thank our anonymous reviewers for their helpful feedback on the manuscript.

664 **References**

1. C. X. Cunningham, G. J. Williamson, D. M. J. S. Bowman, Increasing frequency and intensity of the most extreme wildfires on Earth. Nat Ecol Evol 8, 1420–1425 (2024).

2. G. R. Van Der Werf, et al., Global fire emissions estimates during 1997-2016. Earth Syst Sci Data 9, 697–720 (2017).

3. D. G. Neary, C. C. Klopatek, L. F. DeBano, P. F. Ffolliott, Fire effects on belowground sustainability: a review and synthesis. For Ecol Manage 122, 51–71 (1999).

4. L. E. Nave, E. D. Vance, C. W. Swanston, P. S. Curtis, Fire effects on temperate forest soil C and N storage. Ecological Applications 21, 1189–1201 (2011).

5. S. R. Dooley, K. K. Treseder, The effect of fire on microbial biomass: A meta-analysis of field studies. Biogeochemistry 109, 49–61 (2012).

6. Y. Pressler, J. C. Moore, M. F. Cotrufo, Belowground community responses to fire: meta-analysis reveals contrasting responses of soil microorganisms and mesofauna. Oikos 128, 309–327 (2019).

7. S. Fox, et al., Fire as a driver of fungal diversity — A synthesis of current knowledge. Mycologia 114, 215–241 (2022).

8. B. M. Goodridge, et al., Retention of nitrogen following wildfire in a chaparral ecosystem. Ecosystems 21, 1608–1622 (2018).

9. P. C. Campbell, et al., Pronounced increases in nitrogen emissions and deposition due to the historic 2020 wildfires in the western U.S. Science of The Total Environment 839, 156130 (2022).

10. C. Santín, S. H. Doerr, C. M. Preston, G. González-Rodríguez, Pyrogenic organic matter production from wildfires: a missing sink in the global carbon cycle. Glob Chang Biol 21, 1621–1633 (2015).

11. A. A. Malik, et al., Bacterial population-level trade-offs between drought tolerance and resource acquisition traits impact decomposition. ISME J 18, 224 (2024).

12. D. J. Enright, K. M. Frangioso, K. Isobe, D. M. Rizzo, S. I. Glassman, Mega-fire in redwood tanoak forest reduces bacterial and fungal richness and selects for pyrophilous taxa that are phylogenetically conserved. Mol Ecol 31, 2475–2493 (2022).

13. T. Whitman, et al., Soil bacterial and fungal response to wildfires in the Canadian boreal forest across a burn severity gradient. Soil Biol Biochem 138, 107571 (2019).

14. J. P. Grime, Evidence for the Existence of three primary strategies in plants and its relevance to ccological and evolutionary theory. Am Nat 111, 1169–1194 (1977).

15. M. F. Pulido-Chavez, et al., Rapid bacterial and fungal successional dynamics in first year after chaparral wildfire. Mol Ecol 32, 1685–1707 (2023).

16. N. Lustenhouwer, et al., A trait-based understanding of wood decomposition by fungi. Proc Natl Acad Sci U S A 117, 11551–11558 (2020).

17. T. Camenzind, et al., Towards establishing a fungal economics spectrum in soil saprobic fungi. Nat Commun 15, 1–13 (2024).

18. J. E. Stajich, Fungal genomes and insights into the evolution of the kingdom. Microbiol Spectr 5 (2017).

19. E. Gluck-Thaler, et al., Giant starship elements mobilize accessory genes in fungal genomes. Mol Biol Evol 39 (2022).

20. A. S. Steindorff, et al., Diversity of genomic adaptations to the post-fire environment in Pezizales fungi points to crosstalk between charcoal tolerance and sexual development. New Phytol 236, 1154–1167 (2022).

21. A. S. Steindorff, et al., Comparative genomics of pyrophilous fungi reveals a link between fire events and developmental genes. Environ Microbiol 23, 99–109 (2021).

22. I. Wapinski, A. Pfeffer, N. Friedman, A. Regev, Natural history and evolutionary principles of gene duplication in fungi. Nature 449, 54–61 (2007).

23. M. A. Ciach, J. Pawłowska, P. Górecki, A. Muszewska, The interkingdom horizontal gene transfer in 44 early diverging fungi boosted their metabolic, adaptive, and immune capabilities. Evol Lett 8, 526–538 (2024).

24. D. J. Enright, et al., Evaluating best practices for isolating pyrophilous bacteria and fungi from burned soil. bioRxiv 2024.09.16.612975 (2024). https://doi.org/10.1101/2024.09.16.612975.

25. M. V. Caiafa, et al., Distinct fungal and bacterial responses to fire severity and soil depth across a ten-year wildfire chronosequence in beetle-killed lodgepole pine forests. For Ecol Manage 544, 121160 (2023).

26. H. Suenaga, et al., Novel organization of aromatic degradation pathway genes in a microbial community as revealed by metagenomic analysis. ISME J 3, 1335–1348 (2009).

27. D. J. Levy-Booth, et al., Genomics and metatranscriptomics of biogeochemical cycling and degradation of lignin-derived aromatic compounds in thermal swamp sediment. ISME J 15, 879–893 (2020).

28. A. R. Nelson, et al., Wildfire-dependent changes in soil microbiome diversity and function. Nat Microbiol 7, 1419–1430 (2022).

29. G. Fuchs, M. Boll, J. Heider, Microbial degradation of aromatic compounds — from one strategy to four. Nat Rev Microbiol 9, 803–816 (2011).

30. C. Park, J. Zhang, High expression hampers horizontal gene transfer. Genome Biol Evol 4, 523–532 (2012).

31. A. J. McCarthy, et al., Extensive horizontal gene transfer during Staphylococcus aureus co-colonization in vivo. Genome Biol Evol 6, 2697–2708 (2014).

32. B. Auxier, T. Czaran, D. K. Aanen, Modelling the consequences of the dikaryotic life cycle of mushroom-forming fungi on genomic conflict. Elife 11, e75917 (2022).

33. D. S. LeBauer, K. K. Treseder, Nitrogen limitation of net primary productivity in terrestrial ecosystems is globally distributed. Ecology 89, 371–379 (2008).

34. J. Lehmann, et al., Persistence of soil organic carbon caused by functional complexity. Nat Geosci 13, 529–534 (2020).

35. T. D. Bruns, J. A. Chung, A. A. Carver, S. I. Glassman, A simple pyrocosm for studying soil microbial response to fire reveals a rapid, massive response by Pyronema species. PLoS One 15, e0222691 (2020).

36. M. F. Pulido Barriga, A. N. Kuhn, P. M. Homyak, M. J. Wilkins, S. I. Glassman, Chaparral wildfire shifts the functional potential for soil pyrogenic organic matter and nitrogen cycling. Soil Biol Biochem 211, 109985 (2025).

37. J. Houbraken, et al., Classification of Aspergillus, Penicillium, Talaromyces and related genera (Eurotiales): An overview of families, genera, subgenera, sections, series and species. Stud Mycol 95, 5–169 (2020).

38. J. B. Tanney, K. A. Seifert, Rasamsonia pulvericola sp. nov., isolated from house dust. IMA Fungus 4, 205 (2013).

39. T. K. Kolanlarlı, A. Ahsen, B. Sen, S. Ohten, Biodiversity of Penicillium species isolated from Edirne Söğütlük Forest soil (Turkey). The Journal of Fungus 10, 26–39 (2019).

40. C. F. McRae, R. D. Seppelt, A. D. Hocking, Penicillium species from terrestrial habitats in the Windmill Islands, East Antarctica, including a new species, Penicillium antarcticum. Polar Biol 21, 97–111 (1999).

41. L. W. Kong, et al., Two new antifungal indole alkaloids from an endophytic fungi Aspergillus felis obtained from cigar tobacco. Chem Nat Compd 59, 1132–1136 (2023).

42. G. Mendes, et al., Antifungal activity of extracts from Atacama Desert fungi against Paracoccidioides brasiliensis and identification of Aspergillus felis as a promising source of natural bioactive compounds. Mem Inst Oswaldo Cruz 111, 209–217 (2016).

43. X. Liu, Z. Y. Zhou, J. L. Cui, M. L. Wang, J. H. Wang, Biotransformation ability of endophytic fungi: from species evolution to industrial applications. Appl Microbiol Biotechnol 105, 7095–7113 (2021).

44. Y. L. Huang, M. M. N. Devan, J. M. U'Ren, S. H. Furr, A. E. Arnold, Pervasive effects of wildfire on foliar endophyte communities in Montane forest trees. Microb Ecol 71, 452–468 (2016).

45. D. B. Raudabaugh, et al., Where are they hiding? Testing the body snatchers hypothesis in pyrophilous fungi. Fungal Ecol 43, 100870 (2020).

46. Y. Zhang, P. W. Crous, C. L. Schoch, K. D. Hyde, Pleosporales. Fungal Divers 53, 1–221 (2011).

47. R. Porter, et al., Degradation of polypropylene by fungi Coniochaeta hoffmannii and Pleurostoma richardsiae. Microbiol Res 277, 127507 (2023).

48. R. Riley, et al., Extensive sampling of basidiomycete genomes demonstrates inadequacy of the white-rot/brown-rot paradigm for wood decay fungi. Proc Natl Acad Sci U S A 111, 9923–9928 (2014).

49. A. R. Nelson, et al., Soil microbiome feedbacks during disturbance-driven forest ecosystem conversion. ISME J 18: wrae047 (2024).

50. Z. Merényi, et al., Genomes of fungi and relatives reveal delayed loss of ancestral gene families and evolution of key fungal traits. Nat Ecol Evol 7, 1221–1231 (2023).

51. E. Shahsavari, A. Aburto-Medina, M. Taha, A. S. Ball, A quantitative PCR approach for quantification of functional genes involved in the degradation of polycyclic aromatic hydrocarbons in contaminated soils. MethodsX 3, 205 (2016).

52. S. Garcia-Vallvé, A. Romeu, J. Palau, Horizontal gene transfer of glycosyl hydrolases of the rumen fungi. Mol Biol Evol 17, 352–361 (2000).

53. B. Owens, Fungi borrowed bacterial gene again and again. Nature (2014). https://doi.org/10.1038/NATURE.2014.15496.

54. Y. Wang, et al., Molecular dating of the emergence of anaerobic rumen fungi and the impact of laterally acquired genes. mSystems 4, 10.1128/ (2019).

55. A. A. Hoffmann, Y. Willi, Detecting genetic responses to environmental change. Nat Rev Genet 9, 421–432 (2008).

56. J. M. Talbot, et al., Endemism and functional convergence across the North American soil mycobiome. Proc Natl Acad Sci U S A 111, 6341–6346 (2014).

57. D. Carter-House, J. E Stajich, S. Unruh, T. Kurbessoian, Fungal CTAB DNA Extraction v1. (2020). https://doi.org/10.17504/PROTOCOLS.IO.BHX8J7RW.

58. H. Cheng, G. T. Concepcion, X. Feng, H. Zhang, H. Li, Haplotype-resolved de novo assembly using phased assembly graphs with hifiasm. Nat Methods 18, 170–175 (2021).

59. S. Nurk, et al., HiCanu: Accurate assembly of segmental duplications, satellites, and allelic variants from high-fidelity long reads. Genome Res 30, 1291–1305 (2020).

60. M. Kolmogorov, J. Yuan, Y. Lin, P. A. Pevzner, Assembly of long, error-prone reads using repeat graphs. Nat Biotech 37, 540–546 (2019).

61. A. Gurevich, V. Saveliev, N. Vyahhi, G. Tesler, QUAST: quality assessment tool for genome assemblies. Bioinformatics 29, 1072–1075 (2013).

62. M. Manni, M. R. Berkeley, M. Seppey, E. M. Zdobnov, BUSCO: Assessing genomic data quality and beyond. Curr Protoc 1, e323 (2021).

63. A. V. Zimin, et al., Hybrid assembly of the large and highly repetitive genome of Aegilops tauschii, a progenitor of bread wheat, with the MaSuRCA mega-reads algorithm. Genome Res 27, 787–792 (2017).

64. J. T. Robinson, et al., Integrative genomics viewer. Nat Biotech 29, 24–26 (2011).

65. P. Edge, V. Bafna, V. Bansal, HapCUT2: robust and accurate haplotype assembly for diverse sequencing technologies. Genome Res 27, 801–812 (2017).

66. G. Marçais, et al., MUMmer4: A fast and versatile genome alignment system. PLoS Comput Biol 14, e1005944 (2018).

806 67. M. I. Love, W. Huber, S. Anders, Moderated estimation of fold change and dispersion for RNA-seq
807 data with DESeq2. Genome Biol 15, 1–21 (2014).

808 68. B. Min, I. V. Grigoriev, I. G. Choi, FunGAP: Fungal Genome Annotation Pipeline using evidence-
809 based gene model evaluation. Bioinformatics 33, 2936–2937 (2017).

810 69. P. Jones, et al., InterProScan 5: genome-scale protein function classification. Bioinformatics 30,
811 1236–1240 (2014).

812 70. K. Riehl, C. Riccio, E. A. Miska, M. Hemberg, TransposonUltimate: software for transposon
813 classification, annotation and detection. Nucleic Acids Res 50, e64–e64 (2022).

814 71. P. F. Chuckran, et al., Rapid response of nitrogen cycling gene transcription to labile carbon
815 amendments in a soil microbial community. mSystems 6, 10.1128 (2021).

816 72. T. A. Patrick, L. W. Maguire, J. Espin, C. M. Gardner, Wildfire impacts on soil microbiomes:
817 potential for disruptions to nitrogen-cycling bacteria. Environ Eng Sci 41, 337–346 (2024).

818 73. H. G. Hoang, et al., The nitrogen cycle and mitigation strategies for nitrogen loss during organic
819 waste composting: A review. Chemosphere 300, 134514 (2022).

820 74. S. A. Higgins, et al., Detection and diversity of fungal nitric oxide reductase genes (p450nor) in
821 agricultural soils. Appl Environ Microbiol 82, 2919–2928 (2016).

822 75. F. Sievers, D. G. Higgins, Clustal Omega for making accurate alignments of many protein
823 sequences. Prot Sci 27, 135–145 (2018).

824 76. H. Tang, et al., JCVI: A versatile toolkit for comparative genomics analysis. iMeta 3, e211 (2024).

825 77. D. M. Emms, S. Kelly, OrthoFinder: Phylogenetic orthology inference for comparative genomics.
826 Genome Biol 20, 1–14 (2019).

827 78. R Core Team, R: A Language and environment for statistical computing. R Foundation for
828 Statistical Computing, Vienna, Austria (2023).

829 79. L. J. Revell, phytools: an R package for phylogenetic comparative biology (and other things).
830 Methods Ecol Evol 3, 217–223 (2012).

831 80. D. Kim, J. M. Paggi, C. Park, C. Bennett, S. L. Salzberg, Graph-based genome alignment and
832 genotyping with HISAT2 and HISAT-genotype. Nat Biotechnol 37, 907–915 (2019).

833 81. R. V. Alvarez, L. S. Pongor, L. Mariño-Ramírez, D. Landsman, TPMCalculator: one-step software to
834 quantify mRNA abundance of genomic features. Bioinformatics 35, 1960–1962 (2019).

835 82. Z. Zhang, et al., KaKs_Calculator: Calculating Ka and Ks through model selection and model
836 averaging. Genomics Proteomics Bioinform 4, 259–263 (2006).

837 83. E. Sari, et al., Strain-level adaptation of pyrophilous bacteria through gene fragmentation and
838 horizontal gene transfer. bioRxiv 2025.11.11.687939 (2025).
839 https://doi.org/10.1101/2025.11.11.687939.

84. G. R. Warnes, et al., gplots: Various R programming tools for plotting data. R package version 2, 1 (2009).

85. Hollander M, Wolfe DA, Chicken E (2013) Nonparametric Statistical Methods, 3rd Ed. (Wiley, Hoboken, NJ).

86. M. Friendly, Corrgrams. Am Stat 56, 316–324 (2002).

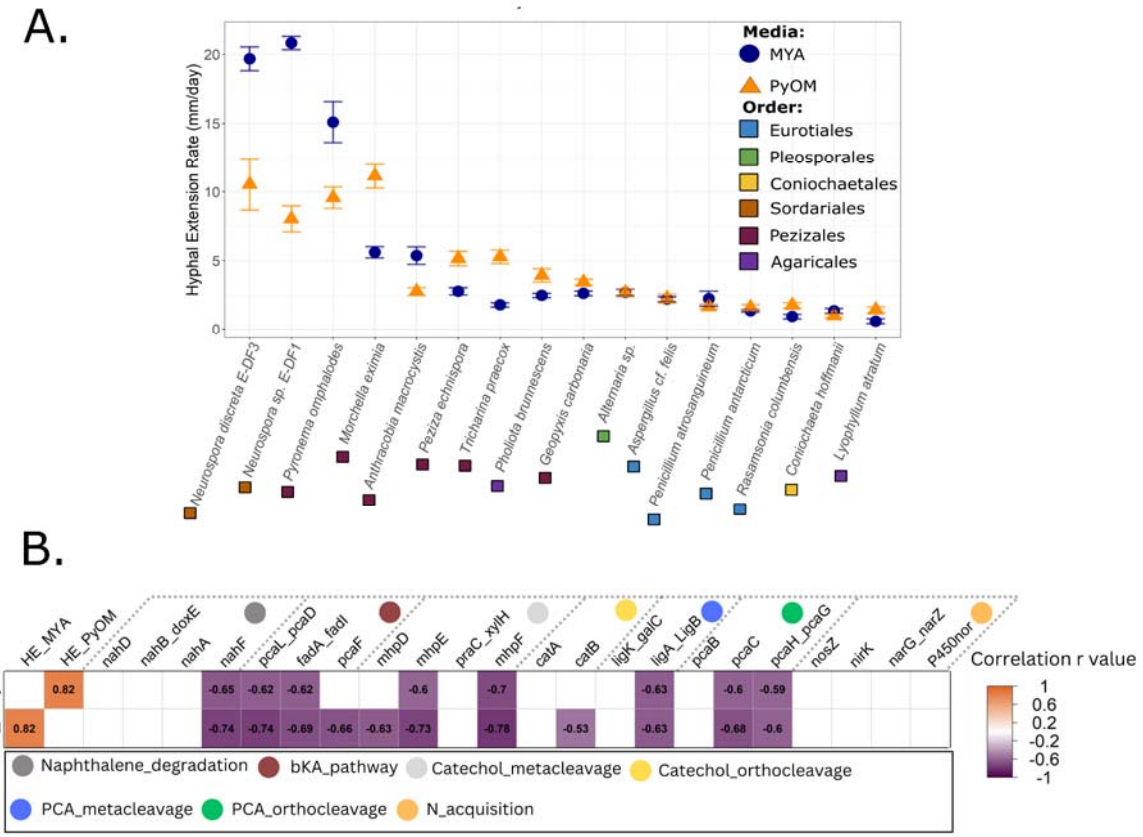

Fig 1. Hyphal extension of 16 pyrophilous fungi on Malt Yeast extract Agar (MYA) and Pyrogenic Organic Matter (PyOM) media **(A)** and pairwise Spearman's rank correlation between the hyphal extension on MYA (HE_MYA) and PyOM (HE_PyOM) media and the number of aromatic C degradation and N acquisition orthologues in each isolate **(B)**. Error bars in panel A shows standard errors of mean. Number in the cells denote pair-wise correlation r values. Gene abbreviation in panel B; nahD: 2-hydroxychromene-2-carboxylate-isomerase, nahB_doxE: cis-1,2-dihydro-1,2-dihydroxy naphthalene, nahA: Naphthalene-1,2-dioxygenase subunit-alpha, nahF: salicylaldehyde_dehydrogenase, pcaL_pcaD: 3-oxoadipate-enol-lactonase, fadA_fadI:Acetyl-Co A acyltransferase, pcaF: beta-ketoadipyl-CoA-thiolase, mhpD: 2-keto-4-pentenoate hydratase, mhpE: hydroxy_oxovalerate_aldolase, praC_xylH: 4-oxalocrotonate_tautomerase, mhpF: acetaldehyde_dehydrogenase, catA: catechol-1,2-dioxygenase, catB: muconate cycloisomerase, ligK_galC: 4-hydroxy-4-methyl-2-oxoglutarate aldolase, ligA_LigB: Protocatechuate-dioxygenase, pcaB: 3-carboxy-cis,cis-muconate-cycloisomerase, pcaC: 4-carboxy muconolactone-decarboxylase, pcaH_pcaG: Protocatechuate-3,4-dioxygenase, nosZ: nitrous-oxide-reductase, nirK: nitrite-reductase; narG_narZ: nitrate-reductase, P450nor: P450 nitric oxide reductase.

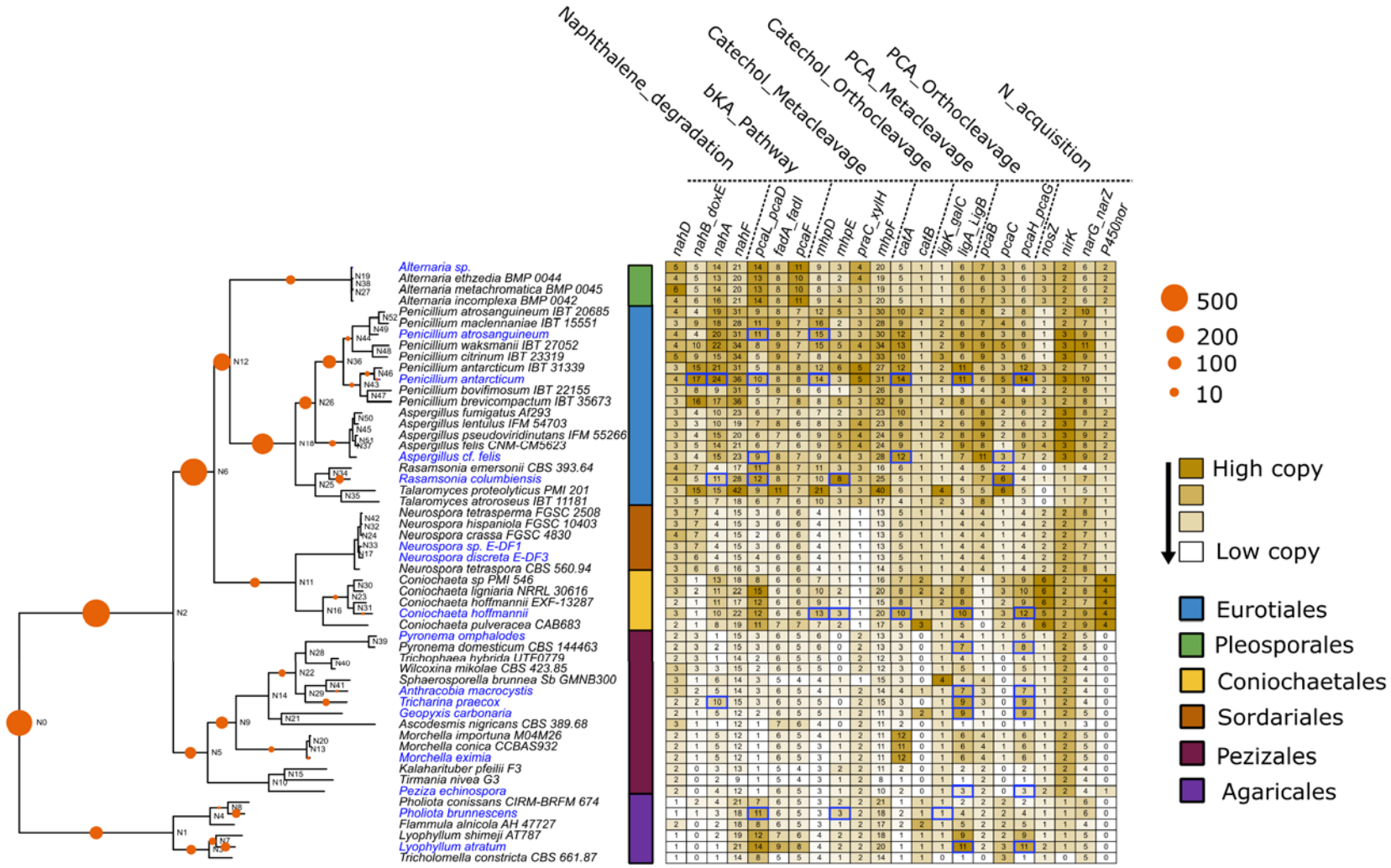

Fig 2. Number of duplication events (orange circles on the species tree) in the aromatic carbon (C) degradation (six pathways) and nitrogen (N) acquisition orthologues in 53 genomes used for constructing orthogroups and their common ancestors vs. the total number of orthologues of 18 aromatic C degradation and four N acquisition genes. The tree leaves printed in blue are 16 pyrophilous species sequenced in this study. The blue

rectangles show significant ($P<0.05$) gene enrichment in pyrophilous vs. non-pyrophilous sister species inferred from Poisson distribution test. Gene name abbreviations: nahD: 2-hydroxychromene-2-carboxylate-isomerase, nahB_doxE: cis-1,2-dihydro-1,2-dihydroxy naphthalene, nahA: Naphthalene-1,2-dioxygenase subunit-alpha, nahF: salicylaldehyde_dehydrogenase, pcaL_pcaD: 3-oxoadipate-enol-lactonase, fadA_fadI: Acetyl-Co A acyltransferase, pcaF: beta-ketoadipyl-CoA-thiolase, mhpD: 2-keto-4-pentenoate hydratase, mhpE: hydroxy_oxovalerate_aldolase, praC_xylH: 4-oxalocrotonate_tautomerase, mhpF: acetaldehyde_dehydrogenase, catA: catechol-1,2-dioxygenase, catB: muconate cycloisomerase, ligK_galC: 4-hydroxy-4-methyl-2-oxoglutarate aldolase, ligA_LigB: Protocatechuate-dioxygenase, pcaB: 3-carboxy-cis,cis-muconate-cycloisomerase, pcaC: 4-carboxy muconolactone-decarboxylase, pcaH_pcaG: Protocatechuate-3,4-dioxygenase, nosZ: nitrous-oxide-reductase, nirK: nitrite-reductase; narG_narZ: nitrate-reductase, P450nor: P450 nitric oxide reductase.

1

A.

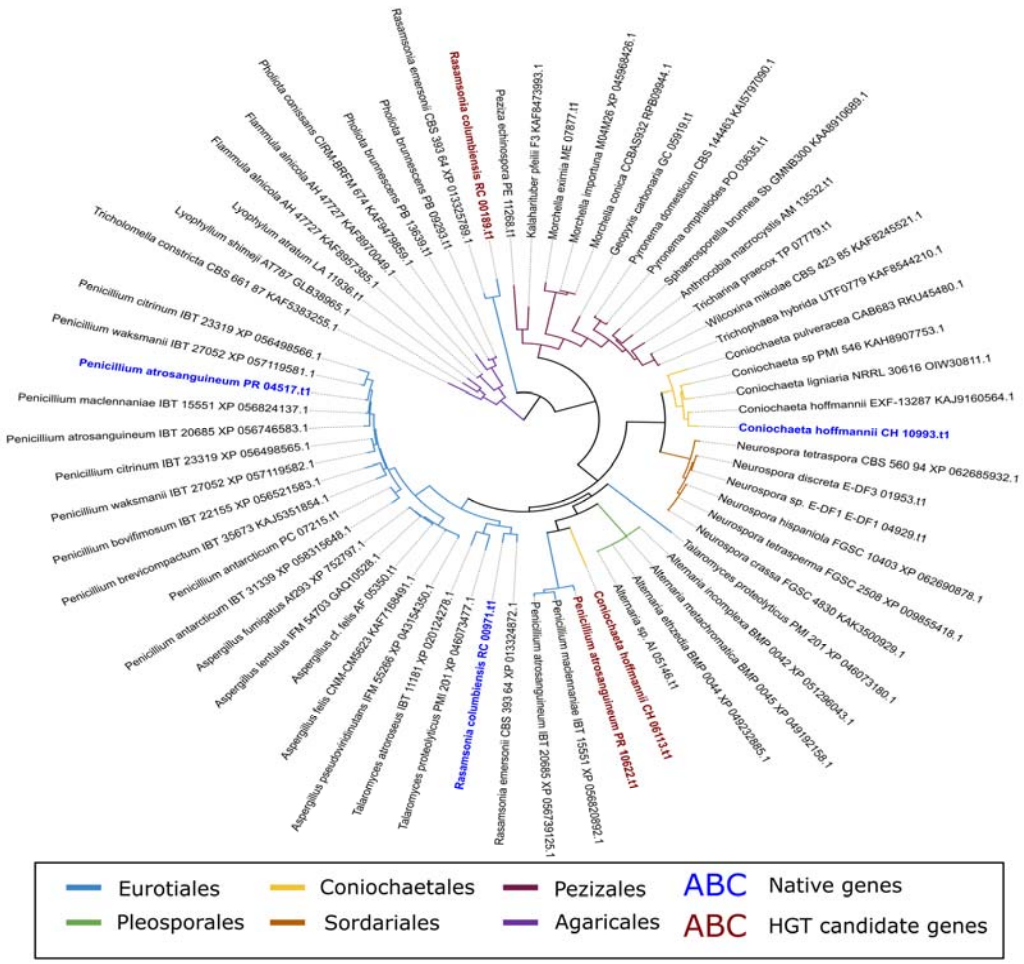
Rasamsonia emersonii CBS 393 64 XP 013325789.1
Rasamsonia columbiensis RC 00189.t1
Pazizza echinospora PE 11268.t1
Kalaharituber pfeilii F3 KAF8473993.1
Morchella exima ME 07877.t1
Morchella importuna M04426 XP 045969426.1
Morchella conica CCBAS932 RPB29944.1
Geopyxis calosporia GC 059110.t1
Pyronema domesticum CBS 144463 KAI5797090.1
Pyronema omphalodes PO 03635.t1
Sphaerosporella brunnea Sb GMNB300 KAA8910889.1
Anthracobia macrocystis AM 13532.t1
Tricharina praecox TP 07779.t1
Wilcoxina mikolae CBS 423 85 KAF8245521.1
Trichophaea hybrida UTF0779 KAF8544210.1
Coniochaeta pulveracea CAB683 RKU45480.1
Coniochaeta sp PMI 546 KAH8907753.1
Coniochaeta ligniaria NRRL 30616 OIW30811.1
Coniochaeta hoffmannii EXF-13287 KAJ9160564.1
Coniochaeta hoffmannii CH 10993.t1
Neurospora tetraspora CBS 560 94 XP 062685932.1
Neurospora discreta E-DF3 01953.t1
Neurospora sp. E-DF1 E-DF1 04929.t1
Neurospora hispaniola FGSC 10403 XP 062690878.1
Neurospora crassa FGSC 4830 KAK3500929.1
Neurospora tetrasperma FGSC 2508 XP 009855418.1
Talaromyces proteolyticus PMI 201 XP 046073180.1
Alternaria incomplexa BMP 0042 XP 051296043.1
Alternaria metachromatica BMP 0045 XP 049192158.1
Alternaria ethzedia BMP 0044 XP 049232885.1
Alternaria sp. AI 05146.t1
Coniochaeta hoffmannii CH 06113.t1
Penicillium atrosanguineum PR 10622.t1
Penicillium macleannaniae IBT 15551 XP 056820992.1
Penicillium atrosanguineum IBT 20685 XP 056739125.1
Rasamsonia emersonii CBS 393 64 XP 013324872.1
Rasamsonia columbiensis RC 00971.t1
Talaromyces proteolyticus PMI 201 XP 046073477.1
Talaromyces atroroseus IBT 11181 XP 020124278.1
Aspergillus pseudoviridinutans IFM 55266 XP 043154359.1
Aspergillus feiis CNM-CM5923 KAF7169491.1
Aspergillus cf. feiis AF 05350.t1
Aspergillus lentulus IFM 54703 GAO10528.1
Aspergillus fumigatus Af293 XP 752797.1
Penicillium antarcticum IBT 31339 XP 058315648.1
Penicillium antarcticum PC 07215.t1
Penicillium brevicompactum IBT 35673 KAJ5351854.1
Penicillium bovifimosum IBT 22155 XP 056521583.1
Penicillium waksmanii IBT 27052 XP 057119582.1
Penicillium citrinum IBT 23319 XP 056498565.1
Penicillium atrosanguineum IBT 20685 XP 056746583.1
Penicillium macleannaniae IBT 15551 XP 056824137.1
Penicillium atrosanguineum PR 04517.t1
Penicillium waksmanii IBT 27052 XP 057119581.1
Penicillium citrinum IBT 23319 XP 056498566.1
Tricholomella constricta CBS 661 87 KAF5383255.1
Lyophyllum atratum LA 11936.t1
Lyophyllum shimeji AT787 GLB38965.1
Flammula alnicola AH 47727 KAF8957385.1
Flammula alnicola AH 47727 KAF8970049.1
Phoxida bruneoconis PB 13639.t1
Phoxida bruneoconis PB 09293.t1
Phoxida conissans CIRM-BREM 874 KAF9478859.1
Eurotiales
Pleosporales
Coniochaetales
Sordariales
Pezizales
Agaricales
ABC Native genes
ABC HGT candidate genes

B.

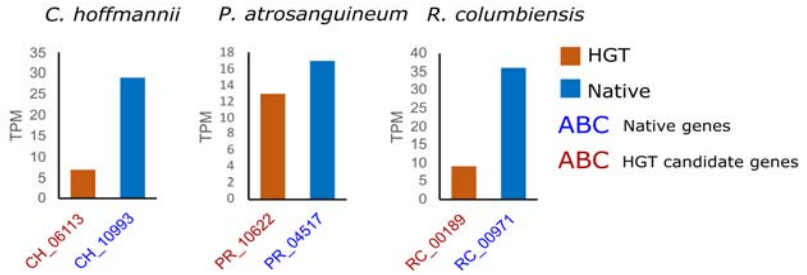
C. hoffmannii
P. atrosanguineum
R. columbiensis
TPM
CH_06113
CH_10993
PR_10622
PR_04517
RC_00189
RC_00971
HGT
Native
ABC Native genes
ABC HGT candidate genes

C.

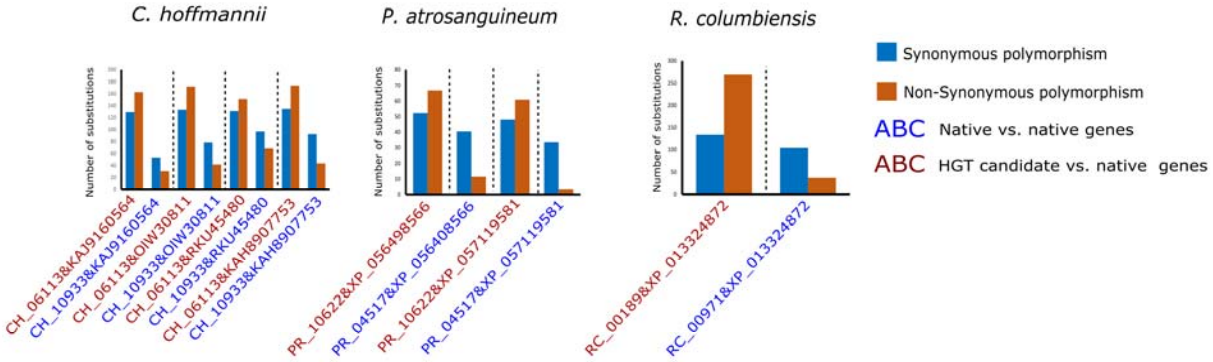
C. hoffmannii
P. atrosanguineum
R. columbiensis
Number of substitutions
CH_061138&KAJ9160564
CH_109338&KAJ9160564
CH_061138&OIW30811
CH_109338&OIW30811
CH_061138&RKU45480
CH_109338&RKU45480
CH_061138&KAH8907753
CH_109338&KAH8907753
PR_106228&XP_056498566
PR_045178&XP_056408566
PR_106228&XP_057119581
PR_045178&XP_057119581
RC_001898&XP_013324872
RC_009718&XP_013324872
Synonymous polymorphism
Non-Synonymous polymorphism
ABC Native vs. native genes
ABC HGT candidate vs. native genes

Fig 3. The Evidence supporting a horizontal gene transfer (HGT) event in OG0001245 orthogroup, described as catechol-1,2-dioxygenase (*catA*) in three pyrophilous species *Coniochaeta hoffmannii*, *Penicillium atrosanguineum*, and *Rasamsonia columbiensis*. Gene tree containing the 63 orthologues of OG0001245 orthogroups **(A),** the transcription (transcript per million [TPM]) values of the candidate HGT genes and their native paralogues **(B)**, and the number of synonymous and non-synonymous nucleotide polymorphisms within the candidate HGT gene and their native paralogues vs. native orthologues of sister species **(C)**.

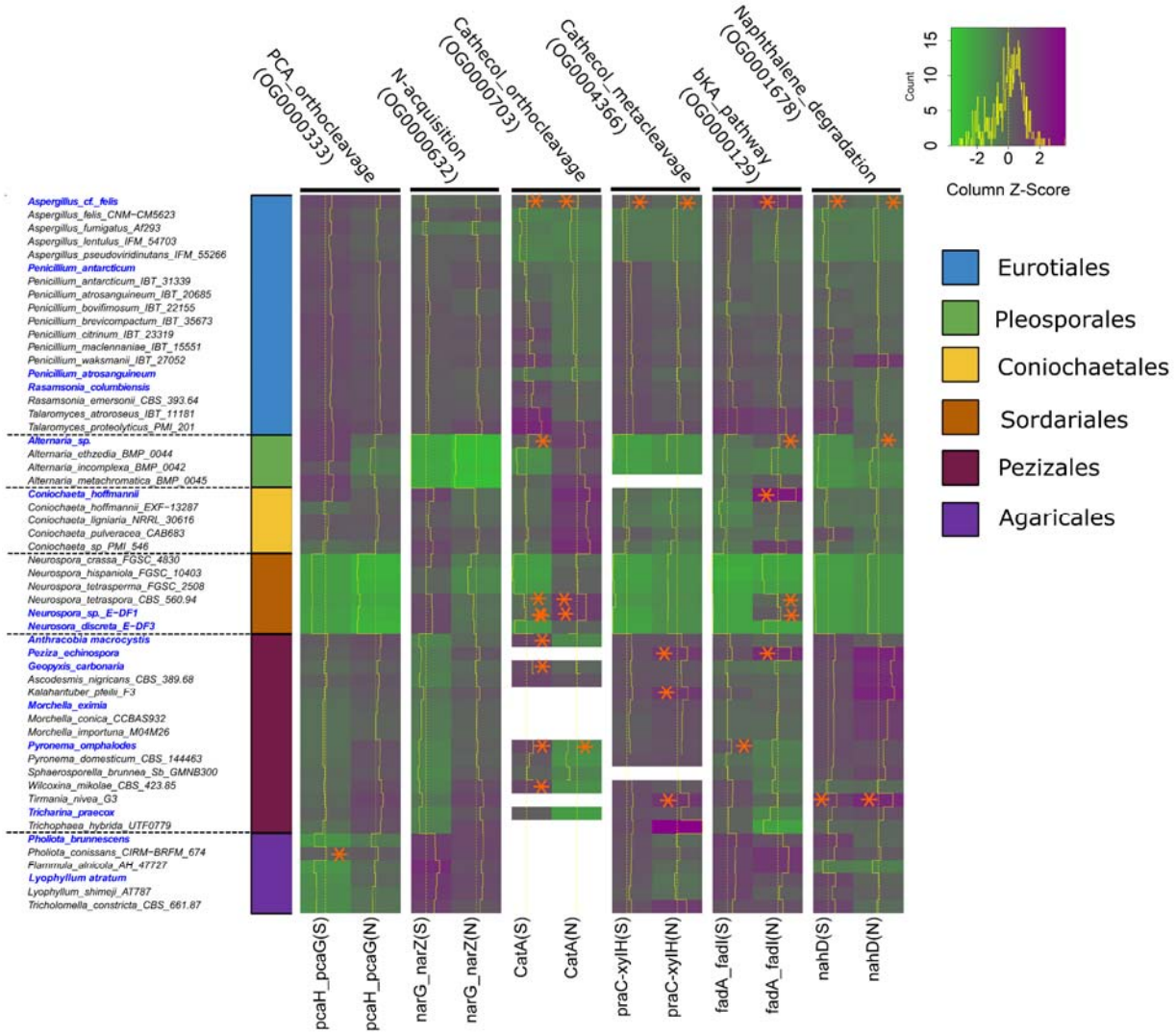

Fig 4. The number of synonymous and nonsynonymous nucleotide substitution in six orthogroups representing five aromatic C degradation and the N acquisition pathways in 53 genomes used for orthogroup construction. Taxa in blue text were sequenced in this study. The dash line in each heatmap cell shows the median number of nucleotide polymorphisms across all taxa for each orthogroups and the solid line is that of each taxon. The heat map color scale represents nucleotide substitution counts for each orthologue, with green indicating lower and purple indicating higher frequencies. The labels at the top of the heat map denote the names of selected orthogroups from each pathway, while those at the bottom indicate gene names and whether the substitutions are synonymous (S) or nonsynonymous (N). The stars denote significantly higher ($P < 0.05$) number of genetic variants in pyrophilous than their non-pyrophilous sister species inferred from Poisson distribution test. Orthogroups selected were described as Protocatechuate-3,4-dioxygenase (*pcaH_pcaG*), nitrate reductase (*narG-narZ*), catechol-1,2-dioxygenase (*catA*), 4-oxalocrotonate tautomerase (*praC-xylH*), Acetyl-Co A acyltransferase (*fadA_fadI*), and 2-hydroxychromene-2-carboxylate isomerase (*nahD*). White cells in heat-map indicated absence of genes in the corresponding taxa, impeding the calculation of the substation rate.